Journal of Russian Laser Research, Volume 17, Number 3, 1996

ANALYTICAL TECHNIQUE FOR CALCULATION OF MIRROR SURFACE PARAMETERS IN "HEX-DARR" RESONATOR FOR LASERS WITH A RING ACTIVE MEDIUM

A. M. Fedorovskii, A. A. Stepanov, and V. A. Shcheglov

P. N. Lebedev Physical Institute, Russian Academy of Sciences, Leninsky Pr. 53, 117924 Moscow, Russia

Abstract

Within the geometrical optics approximation, we consider a class of mirrors (with surfaces formed by rotating second-order curves) which enables an extension of the range of possible beam conversions in optical systems. The formulas used in the calculations are quite simple. Based on this approach, we worked out and presented a complete analytical algorithm for calculation of the mirror surface parameters in a "HEX-DARR" resonator. To check the algorithm, a numerical calculation of an optical system is carried out for a specific set of initial data. The results obtained confirm the accuracy of the equations derived and the efficiency of the algorithm.

1. Introduction

The choice of a resonator type is of prime importance in the design of lasers with a ring active medium. A description of resonators of several classes applicable in this instance is available in the literature (e.g., see [1]). The "HEX-DARR" resonator is one of the most interesting schemes [2].

The mirror geometry in this resonator has its own special features. As a rule, mirrors of rather simple shapes are used in optics. In optical systems, they are commonly used for collimating convergent/divergent beams or for changing the center of curvature without changing its value. This problem is solved using, respectively, spherical (parabolic) and plane mirrors. With cylindrical optics, similar problems are tackled using mirrors formed by rotating a portion of a circle (parabola) or a straight line. It is a relatively simple matter in this case to reconstruct the mirror shape from the ray traces. A wider range of beam conversions (such as a convergent-to-convergent beam change with variation of curvature and so forth) and, hence, a broader class of mirrors are used in a HEX-DARR resonator.

Accordingly, the problem of determining the mirror shape becomes more complicated. The use of conventional methods based on the paraxial approach and the third-order aberration theory is extremely hampered in this case. In the differential treatment based on the Linneman technique [3], the differential equation is written on the basis of the given beam conversion in reflection by a mirror. Its solution defines a line (as a set of points) – the generatrix of the mirror surface. One of the shortcomings of such an approach is the awkwardness of the result description.

Another method – an analytical one – is the subject of this work. Second order curves are used here to calculate and to represent the mirror surfaces of the resonator. In this case, every mirror is defined by seven parameters in all (five define the shape, and the remaining two, the surface boundaries). We present the calculation results and some useful estimates for a variant of the HEX-DARR resonator with a base length of 2.5 m.

Translated from a manuscript submitted November 29, 1995.

 1071-2836/96/1703-000286$15.00

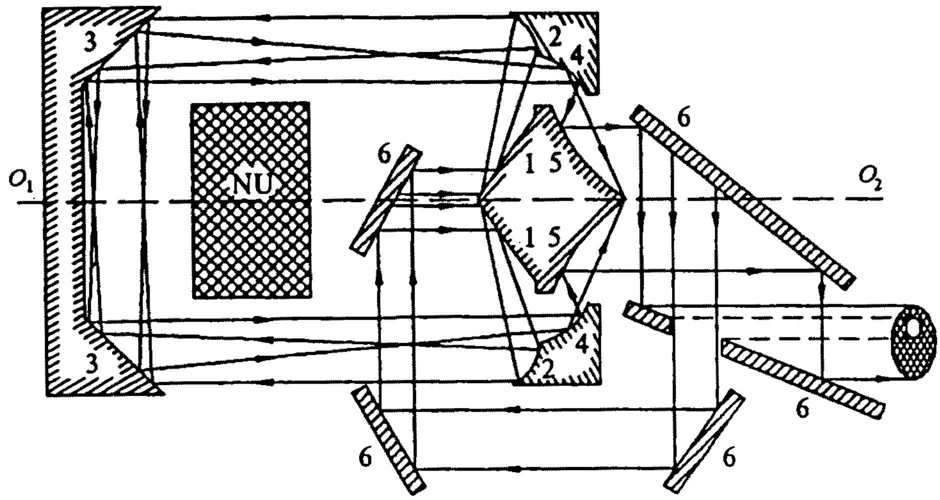

Fig. 1. Schematic of HEX-DARR resonator: nozzle unit (NU); axicones (1–5); plane mirrors (6).

2. Resonator Ray Tracing

The mirror surfaces and the beams themselves are axisymmetric in the HEX-DARR resonator. We will consider our problem in a section through the axis of symmetry. In what follows, for the sake of simplicity, the term "surface" implies a generating surface of the mirror, and "beam," a set of rays in the section plane. Note that in this case the divergent/convergent beam is a beam whose rays intersect at points lying in an axisymmetric circle.

The ray paths in the HEX-DARR resonator (see Fig. 1) can be described as follows. The beam parallel to the symmetry axis is incident on axicone 1. After its reflection, we obtain a divergent/convergent beam. Axicone 2 converts it into a divergent beam. After its reflection from axicone 3, we obtain a parallel beam at almost a right angle to the axis. After the second reflection, we have a convergent beam. Between axicones 4 and 5, the beam becomes divergent again. Finally, after reflection from axicone 5, we obtain a beam parallel to the axis. Note that after the second reflection from axicone 3 the convergence of the pencil of rays is approximate in character (although the focal spot size is very small). A similar situation takes place after subsequent reflections.

3. Features of Second-Order Curves

Inasmuch as second-order curves will be in active use, it is worthwhile to recall some of their features.

(i) They have equations of the type

$$\begin{aligned} r &= \frac{p}{1+e\cos(\varphi-\varphi_0)}, \quad p>0, \quad e\geq 0; \\ x &= x_0 + r\cos\varphi; \\ y &= x_0 + r\sin\varphi; \\ \varphi_1 &< \varphi < \varphi_2, \end{aligned} \tag{1}$$

where (x_0, y_0) are the Cartesian coordinates of the curve focus; φ_0 is the direction of the major curve axis (from the focus to the closest line tip); (r, φ) are the polar coordinates of a curve point relative to the focus. All of the angles are measured counterclockwise from the X axis. The curve type is determined by the value of e :

$$\begin{aligned} 0 = e &\iff \text{a circle;}\\ 0 < e < 1 &\iff \text{an ellipse;}\\ e = 1 &\iff \text{a parabola;}\\ e > 1 &\iff \text{a hyperbola (a short-range branch).} \end{aligned}$$

(ii) Upon reflection from the "inside" (as viewed from the focus), a beam diverging from one focus is transformed by a parabola into a beam parallel to the major axis, by an ellipse into a beam converging to another focus, and by a hyperbola into a beam diverging from another focus (the angular beam size decreases). A beam parallel to the major axis is converted by a parabola into a beam converging to a focus.

Upon reflection from the "outside," a beam converging to one focus is transformed by a parabola into a beam parallel to the major axis, by an ellipse into a beam diverging from another focus, and by a hyperbola into a beam converging to another focus (the angular beam size increases). A beam parallel to the major axis is converted by a parabola into a beam diverging from a focus.

Note that, as shown below, the above-stated property of converting a spherical wave to a spherical or plane ones is displayed in reflection only by second-order curves and straight lines.

(iii) For an ellipse, the sum of distances to the foci is constant:

$$r_1 + r_2 = \text{const.}$$

For a hyperbola, the difference between distances to the foci is constant:

$$r_1 - r_2 = \text{const.}$$

(iv) The direction of the normal to a parabola φ_n :

$$\varphi_n - \varphi_0 = \frac{\varphi_n - \varphi_0}{2} \Rightarrow \varphi = 2\varphi_n - \varphi_0.$$

The relationship between the angles for reflection:

$$\varphi_n - \varphi_1 = \varphi_2 + \pi - \varphi_n \Rightarrow 2\varphi_n = \varphi_1 + \varphi_2 + \pi,$$

where φ_1 and φ_2 are the angles of inclination of the ray before and after reflection. Consequently,

$$\varphi = \varphi_1 + \varphi_2 + \pi - \varphi_0. \tag{2}$$

(v) For a parabola with $\varphi_0 = 0$,

$$y - y_0 = p\,\frac{\sin\varphi}{1 + \cos\varphi} = p\tan\varphi/2\,. \tag{3}$$

For a parabola with $\varphi_0 = \pi$,

$$y - y_0 = p\,\frac{\sin\varphi}{1 - \cos\varphi} = \frac{p}{\tan\varphi/2}\,. \tag{4}$$

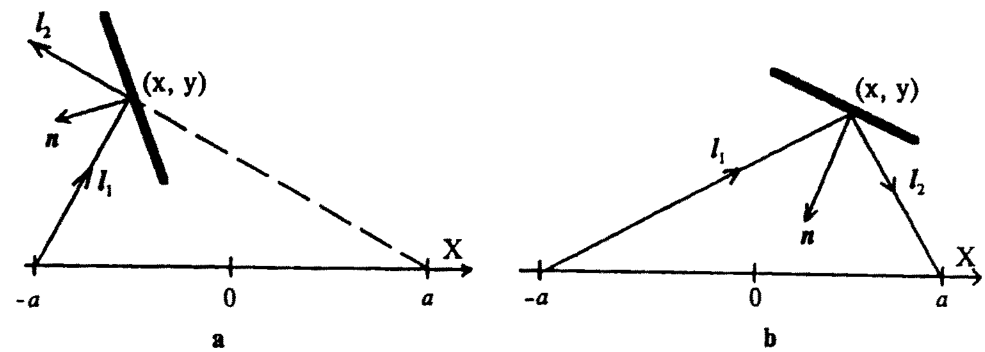

Fig. 2. Ray traces for reflection from mirror: "external" reflection (a); "internal" reflection (b).

4. General Form of an Axicone

We obtain the general form of a curve exhibiting the following property: a beam diverging from one focus diverges/converges to another after reflection (see Fig. 2).

We introduce a system of Cartesian coordinates with its origin in the middle of the segment connecting the foci. The X axis is directed from the first focus to the second. We denote the interfocal distance by $2a > 0$. The direction vector of the beam before reflection is symbolized as $\mathbf{l}_1$, after reflection as $\mathbf{l}_2$, and the normal at the point of incidence as $\mathbf{n}$.

From the law of reflection

$$\mathbf{l}_2\mathbf{n} = \mathbf{l}_1\mathbf{n}.$$

We require, in addition, that

$$|\mathbf{l}_2| = |\mathbf{l}_1|.$$

Then, expanding vector $\mathbf{l}_2$ into vectors $\mathbf{l}_1$ and $\mathbf{n}$, it is readily found that

$$\mathbf{l}_2 = \mathbf{l}_1 + b\mathbf{n},$$

where

$$b = -\frac{2\mathbf{n}\mathbf{l}_1}{|\mathbf{n}|^2}.$$

Let (x, y) be the coordinates of the incidence point. Then,

$$\begin{aligned}\mathbf{l}_1 &= (x + a, y);\\ \mathbf{n} &= (dy, -dx).\end{aligned}$$

From obvious geometric considerations, we have

$$(x - a, y) = \text{const}\,\mathbf{l}_2 = \text{const}\,[(x + a) + b\,dy,\ y - b\,dx].$$

Eliminating const, we obtain

$$(x - a)(y - b\,dx) = y\,[(x + a) + b\,dy].$$

Substitution of the value of b gives

$$dx\,dy\,(x^2 - a^2 - y^2) = xy\left[(dx)^2 - (dy)^2\right].$$

The equation supports the substitutions

$$x \to -x; \quad y \to -y.$$

Therefore, one can introduce the new variables

$$X = x^2, \quad dX = 2x\,dx;$$
$$Y = y^2, \quad dY = 2y\,dy.$$

With the new variables, the equation takes the form

$$dX\,dY\,(X - Y - a^2) = Y\,(dX)^2 - X\,(dY)^2.$$

If

$$dX = 0,$$

we obtain the obvious solution

$$x = 0.$$

Otherwise, one can introduce

$$Y' = \frac{dY}{dX}.$$

After this, the equation acquires the form

$$Y'\,(X - Y - a^2) = Y - X\,(Y')^2. \tag{5}$$

Differentiating (5) gives

$$Y''\,(X - Y - a^2 + 2XY') = 0.$$

We have two variants. The first one is:

$$Y'' = 0 \quad \Rightarrow \quad Y = AX + B.$$

Substituting into (5), we find the relation between A and B :

$$A = -\frac{B}{B + a^2}.$$

The second variant is:

$$X - Y - a^2 = -2XY'.$$

Substituting into (5), we obtain

$$X\,(Y')^2 = -Y \quad \text{or} \quad (xY')^2 = -y^2.$$

The only solution to this equation

$$y = 0$$

has no physical significance.

So, the solution sought is given by

$$Y = -\frac{BX}{B+a^2} + B \quad \text{or} \quad y^2 = -\frac{Bx^2}{B+a^2} + B.$$

It is easily seen that we obtain a formula for a second-order curve written in Cartesian coordinates. Placing the coordinate origin at one of the foci and directing the polar axis toward the other, we obtain the standard (in polar coordinates) curve form. In so doing, we have two solutions (depending on the sign of B): a hyperbola and an ellipse. In the differential treatment mentioned in the Introduction, these curves are solutions of the differential equation for the generating surface of the mirror.

As the distance to the second focus tends to infinity (the beam is parallel after reflection), we obtain a parabola with passage to the limit. To satisfy the conditions

$$p > 0 \quad \text{and} \quad e \geq 0,$$

is possible for the origin to be transferred to the other focus and/or the direction of the polar axis be reversed.

In summary, an ellipse, a hyperbola, or a straight line converts a beam diverging from one focus into a beam which diverges/converges at the other. The latter can be considered as the limiting case of a hyperbola for

$$e \to \infty \quad \text{and} \quad p = ae.$$

A similar transformation into a parallel beam is performed only by a parabola.

5. Calculation of the Axicone Parameters

From the above, it is easily comprehended that the axicones of the HEX-DARR resonator must be well described in terms of second-order curves. It is an easy matter to obtain the axicone type from the beam type (convergent, divergent, parallel) before and after reflection from the mirror: axicones 1, 3, and 5 are parabolas; axicone 2 is a hyperbola or an ellipse; and axicone 4 is a hyperbola.

In the course of computations, determined for every mirror are the locations of two foci for a hyperbola and an ellipse, and the location of one focus and the axis direction (i.e., φ_0) for a parabola. Additionally, a "reference" point on the line (the point of reflection of the first ray) is determined.

With these data, we next find the parameters p, e, x_0, y_0, and φ_0 according to the following algorithm.

We locate the coordinate origin at the focus nearest to the "reference" point. The polar axis connects the curve foci (for an ellipse and a hyperbola) or is parallel to the axis (for a parabola). In this manner, we calculate the parameters x_0, y_0 and φ_0.

Employing the curve properties (see [4]), it is easy to calculate the parameter e :

$$\begin{array}{lll}
F = 2ae; \quad r_2 + r_1 = 2a \quad \Longrightarrow & e = \dfrac{F}{r_2 + r_1} & \text{for an ellipse;} \\
 & e = 1 & \text{for a parabola;} \\
F = 2ae; \quad r_2 + r_1 = 2a \quad \Longrightarrow & e = \dfrac{F}{r_2 - r_1} & \text{for a hyperbola,}
\end{array}$$

where F is the spacing between line foci; $2a$ is the spacing between line tips; r_1 and r_2 are the distances from the "reference" point to the near and far foci.

It is now easy to calculate the parameter p :

$$p = r_1 - er_1 \cos(\varphi - \varphi_0).$$

Hence, the parameters of a particular axicone are calculated by simple analytical formulas.

Resonator ray tracing imposes obvious geometric limitations on the locations of the axicone foci. With an appropriately chosen set of initial conditions, the locations of the axicone foci (axes) can be uniquely determined and, consequently, the mirror surface shapes can be determined. This problem will be considered in detail.

6. Notation and Initial Data

Let us introduce the coordinate system (X, Y) aligning the X axis with the symmetry axis of the resonator from axicone 3 to axicone 1 and directing the Y axis upwards. We shall examine the ray traces with the beam passing first through the upper section of the resonator and then through the lower one. We introduce the notation:

F_a — the common focus of axicones a and $(a+1)$;

F_{ax}, F_{ay} — the Cartesian coordinates of the focus;

P_{am} — the intersection point of ray m and axicone a;

x_{am}, y_{am} — the Cartesian coordinates of the intersection point;

r_{am}, φ_{am} — the polar coordinates of the intersection point with respect to the axicone focus (for parabolic axicones);

p_a — the parameter p for axicone a;

g_{am} — the inclination angle of ray m to the X axis after reflection from axicone a (for parabolic axicones).

We introduce several refinements of the definitions:

F_3 is the "personal" focus of axicone 4 (the ray convergence point after the second reflection from axicone 3);

F_{-3} is the focus of the lower section of axicone 3;

P_{-3m} and g_{-3m} describe the rays after reflection from the lower section of axicone 3.

The traces of only two outer rays $(y_{11} < y_{12})$ are considered in the calculation. From the resonator ray tracing (see Fig. 1) it is clear that

$$\begin{aligned} g_{22} &= \pi + w; \\ g_{31} &= -\frac{\pi}{2} - q; \\ g_{-31} &= v, \end{aligned}$$

where w, q, and v are small angles.

Different initial data sets can be adopted. Further, a variant with the following initial conditions will be treated:

R_N — the radius of the nozzle unit;

R_L — the radial dimension of the oscillation zone;

R_I — the y-range of the input beam;

R_O — the y-range of the output beam;

X_1 — the x coordinate of the outer edge of axicone 1 $(X_1 = x_{12})$;

X_2 — the x coordinate of the inner edge of axicone 2 $(X_2 = x_{22})$;

X_3 — the x coordinate of the outer edge of axicone 3 $(X_3 = x_{31})$;

R_{24} — the radial clearance between the inner edge of axicone 2 and the outer edge of axicone 4 $(R_{24} = y_{22} - [-y_{41}])$;

R_{3N} — the radial clearance between the beam and the nozzle unit in passing between axicones 3 and 4;

X_{51} — the x-clearance between the outer edges of axicones 5 and 1 ($X_{51} = x_{52} - x_{12}$);
X_{42} — the x-clearance between the outer edge of axicone 4 and the inner edge of axicone 2 ($X_{42} = x_{41} - x_{22}$).

The rays are parallel to the X axis before reflection from axicone 1 and after reflection from axicone 5. Ray 1 between axicones 2 and 3 and ray 2 between axicones 3 and 4 are also parallel to the X axis

$$\begin{aligned} y_{31} &= R_N + R_L; \\ y_{-32} &= -R_N - R_{3N}. \end{aligned}$$

The points of intersection of the rays before and after reflection (also for axicone 4) are assumed to be the axicone foci. In the system presented in Fig. 1, the beam enters the resonator above the axis but emerges below it. Consequently,

$$\begin{aligned} Y_{I1} &\geq 0; & Y_{I2} &> 0; \\ Y_{O1} &\leq 0; & Y_{O2} &< 0. \end{aligned}$$

7. General Computation Scheme

The computation algorithm consists of the three main stages:

(i) Employing a rather good analytical initial approximation (it can be improved by iterations, if necessary) of the parameter q, we calculate the parameters of axicone 3.

(ii) The parameters of axicones 1 and 2 are derived analytically.

(iii) Solving the cubic equation, we find F_{4y}. This enables us to determine all parameters of axicones 4 and 5.

In what follows, the stages of the computation scheme will be considered more closely.

8. Parameters of Axicone 3

In this section, formulas describing ray reflection from axicone 3 (see Fig. 3) will be derived. All quantities considered are first expressed in terms of the parameter q. Next, we obtain an equation in q, which can be solved by iterations.

For the upper section of axicone 3 (a parabola),

$$\begin{aligned} p &= p_3; \\ \varphi_0 &= \frac{\pi}{2} - q; \\ x_0 &= F_{2x}; \\ y_0 &= F_{2y} = R_N + R_L. \end{aligned}$$

Utilizing formulas (1) it is easy to obtain

$$\begin{aligned} r_{31} &= \frac{p_3}{1 - \sin q}; \\ r_{32} &= \frac{p_3}{1 - \sin(q + w)}; \\ x_{31} &= F_{2x} - r_{31}; \\ x_{32} &= F_{2x} - r_{32} \cos w; \\ y_{31} &= F_{2y}; \\ y_{32} &= F_{2y} - r_{32} \sin w. \end{aligned} \tag{6}$$

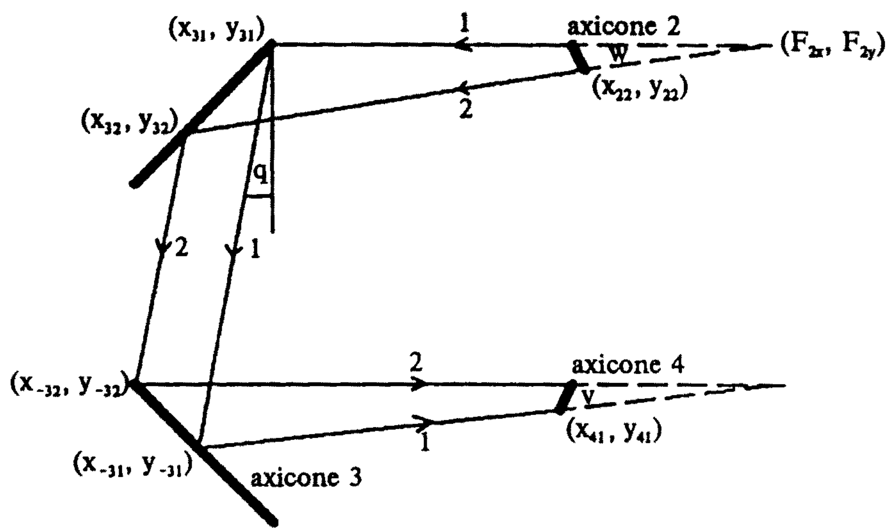

Fig. 3. Reflection of rays from axicone 3.

The lower section of axicone 3 is symmetric to the upper one. In a similar manner, with the additional use of Eq. (2), it is easy to obtain

$$
\begin{aligned}
r_{-31} &= \frac{p_3}{1-\sin(3q-v)}; \\
r_{-32} &= \frac{p_3}{1-\sin 3q}; \\
x_{-31} &= F_{2x} - r_{-31}\cos(2q-v); \\
x_{-32} &= F_{2x} - r_{-32}\cos 2q; \\
y_{-31} &= -F_{2y} + r_{-31}\sin(2q-v); \\
y_{-32} &= -F_{2y} - r_{-32}\sin 2q.
\end{aligned}
\tag{7}
$$

Taking into consideration the inclination of the rays between the two reflections from axicone 3,

$$\frac{x_{-31}-x_{31}}{y_{-31}-y_{31}} = \cot g_{31} - \tan q \tag{8}$$

and

$$\frac{x_{-32}-x_{32}}{y_{-32}-y_{32}} = \cot g_{32} - \tan q. \tag{9}$$

It is seen from the ray tracing that for the inner edge of axicone 2

$$
\begin{aligned}
x_{22} &= F_{2x} - t\cos w; \\
y_{22} &= F_{2y} - t\sin w,
\end{aligned}
$$

while for the outer edge of axicone 4 (in the lower half)

$$\begin{aligned} x_{41} &= x_{-31} + s \cos v; \\ y_{41} &= y_{-31} + s \sin v, \end{aligned}$$

where s and t are some parameters.

So, equations for all the quantities of interest have been obtained.

Let us now take into account the initial data:

$$\begin{aligned} y_{-32} &= -R_N - R_{3N}; \\ F_{2y} &= R_N + R_L. \end{aligned}$$

Then, we readily find from (7) that

$$p_3 = (R_L - R_{3N}) \frac{1 - \sin 3q}{\sin 2q} .$$

Furthermore, in view of $x_{31} = X_3$, we have

$$F_{23} = \frac{X_3 + p_3}{1 - \sin q} .$$

Using Eqs. (8) and (9), expressions for v and w can be obtained:

$$\begin{aligned} v &= 2 \arctan \left(-\frac{A_3}{A_2 + D} \right); \\ w &= -q + 2 \arctan \left[\frac{\sin 3q - (1 - \cos q) - B}{1 + \cos q - \sin 3q - B} \right] , \end{aligned}$$

where

$$\begin{aligned} A_1 &= \cos q \,(1 - \sin q) + (1 + \sin 3q)(\cos q + A); \\ A_2 &= \cos 3q \,(\cos q + A) - \sin q \,(1 - \sin q); \\ A_3 &= \cos q \,(\sin q - \sin 3q) + A(1 - \sin 3q); \\ D &= \sqrt{A_2^2 - A_1 A_3} ; \\ A &= \frac{2F_{2y}}{p_3} \sin q \,(1 - \sin q) ; \\ B &= \frac{2F_{2y}}{p_3} \sin q \,(1 - \sin 3q) . \end{aligned}$$

Finally, taking into account the conditions

$$\begin{aligned} x_{41} - x_{22} &= X_{42}; \\ y_{22} - (-y_{41}) &= R_{24}, \end{aligned}$$

we get:

$$\begin{aligned} s &= \frac{r_{-31} \sin (w + v - 2q) + X_{42} \sin w + R_{24} \cos w}{\sin (w + v)} ; \\ t &= \frac{r_{-31} \sin 2q + X_{42} \sin v - R_{24} \cos v}{\sin (w + v)} . \end{aligned}$$

So, all parameters of axicone 3 are expressed in terms of q. Its value, in turn, can be obtained from the condition

$$x_{22} = X_2.$$

The magnitude of q will be calculated by iterations, minimizing the error $x_{22} - X_2$. Naturally, the problem arises of how to obtain a sufficiently good initial approximation for this parameter. By virtue of its smallness, it would be reasonable to employ an expansion in powers of q.

Let

$$k = 4q\,\frac{R_N + R_L}{R_L - R_{3N}}\,.$$

We point out that

$$\frac{R_N + R_L}{R_L - R_{3N}} \gg 1,$$

but $k = O(1)$ (moreover, typically $k \ll 1$). We expand $x_{22} - X_2$ with relative accuracy $O(q^2)$ and in doing this retain the terms of the order of $O(kq)$. Then, omitting cumbersome intermediate calculations, we obtain the relationship

$$x_{22} - X_2 = \frac{K_2}{q} + K_3(k,q) - K_1 + q\,O\,(R_L - R_{3N} + qX_{42} + R_{24})\,, \tag{10}$$

where

$$\begin{aligned}
K_1 &= X_2 - X_3 + \frac{1}{4}\left[R_L - R_{3N} + 2\,X_{42} + R_{24} + 2\,(R_N + R_L)\left(1 - \frac{R_{24}}{R_L - R_{3N}}\right)\right];\\
K_2 &= \frac{1}{4}\,(R_L - R_{3N} + R_{24});\\
K_3 &= \frac{4}{1 - k/2 + q}\left[(R_L - R_{3N})\left(\frac{k}{2} + q\right) - qX_{42}\left(-2 + \frac{k^2}{2}\right) - R_{24}\left(\frac{k}{2} - q\right)\right.\\
&+ \left.(-k + 2q)(R_N + R_L)\left(1 - \frac{R_{24}}{R_L - R_{3N}}\right)\right].
\end{aligned}$$

With the provision that $x_{22} - X_2 = 0$, relation (10) takes the form

$$q = \frac{K_2}{K_1 - K_3\,(k,q) + q\,O\,(R_L - R_{3N} + qX_{42} + R_{24})}\,.$$

Considering that, as a rule, $K_3 \ll K_1$ we obtain the initial approximation for q in two stages:

(i) $$q_0 = \frac{K_2}{K_1}\,; \quad k_0 = 4q_0\,\frac{R_N + R_L}{R_L - R_{3N}}\,,$$

(ii) $$q_1 = \frac{K_2}{K_1 - K_3\,(k_0, q_0)}\,.$$

Usually, the initial approximations q_0 and q_1 alone provide a wholly acceptable accuracy. If necessary, q can be additionally refined via iterations by the Newton method, starting from $q = q_0$ or $q = q_1$. In so doing, the discrepancy $x_{22} - X_2$ is calculated from the precise analytical equations listed above. The correction for q is found with allowance for the formula

$$\frac{dq}{dX_2} \approx -\frac{K_2}{(K_1 + K_3)^2} \approx -\frac{q^2}{K_2}\,.$$

The iterations converge rapidly.

On obtaining a sufficiently good approximation for q^*, one should set $X_2 = x_{22}\,(q^*)$. If required, the parameters Y_{I1}, Y_{I2}, Y_{O1}, Y_{O2}, X_1, X_5, and X_{51}, which are as yet unused in calculations, can also be modified at this moment.

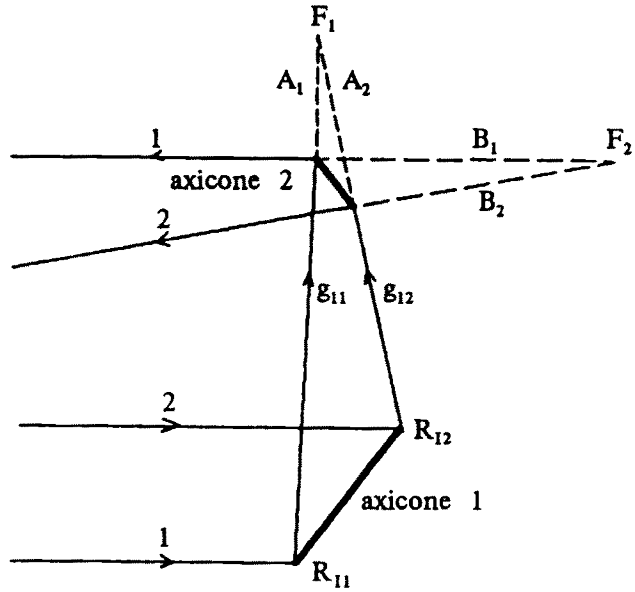

Fig. 4. Reflection of rays from axicones 1 and 2.

9. Parameters of Axicones 1 and 2

This section is dedicated to the derivation of equations for the parameters describing axicones 1 and 2 (see Fig. 4). Note, that x_{22}, y_{22}, F_{2x}, and F_{2y} were obtained previously in the computation of the parameters of axicone 3.

From obvious geometric equations, we have:

$$\tan g_{12} = \frac{y_{22} - Y_{I2}}{x_{22} - X_1} .$$

We introduce the notation:

A_1 and A_2 are the distances from P_{21} and P_{22} to F_1;
B_1 and B_2 are the distances from P_{21} and P_{22} to F_2.

Let the beam converge after reflection from axicone 1. Employing Eqs. (3) and (4), it is readily found that

$$(Y_{I2} - F_{1y}) \tan\left(\frac{g_{12}}{2}\right) = (Y_{I1} - F_{1y}) \tan\left(\frac{g_{11}}{2}\right) . \tag{11}$$

In this case, axicone 2 is an ellipse; therefore,

$$A_1 + B_1 = A_2 + B_2.$$

Taking into account that

$$A_1 = \frac{F_{1y} - y_{21}}{\sin g_{11}} = \frac{F_{1y} - F_{2y}}{\sin g_{11}} ;$$

$$\begin{aligned} A_2 &= \frac{F_{1y} - y_{22}}{\sin g_{12}}; \\ B_1 &= F_{2x} - x_{22} - \frac{F_{1y} - y_{22}}{\tan g_{12}} + \frac{F_{1y} - F_{2y}}{\tan g_{11}}; \\ B_2 &= \sqrt{(F_{1x} - x_{22})^2 + (F_{1y} - y_{22})^2}, \end{aligned}$$

we obtain the relationship

$$(F_{1y} - F_{2y})\left(\frac{1}{\sin g_{11}} + \frac{1}{\tan g_{11}}\right) - (F_{1y} - y_{22})\left(\frac{1}{\sin g_{12}} + \frac{1}{\tan g_{12}}\right) = B_2 - (F_{2x} - x_{22}). \qquad (12)$$

Equations (11) and (12) can be shown to be fulfilled, too, when the beam diverges on reflection from axicone 1 (axicone 2 is a hyperbola).

With the identities

$$\begin{aligned} \frac{1}{\sin x} + \frac{1}{\tan x} &= \frac{1}{\tan x/2}; \\ B_2 - (F_{2x} - x_{22}) &= \frac{(F_{2y} - y_{22})^2}{B_2 + (F_{2x} - x_{22})}, \end{aligned}$$

Equation (12) can be rearranged to give

$$\frac{F_{1y} - F_{2y}}{\tan g_{11}/2} - \frac{F_{1y} - y_{22}}{\tan g_{12}/2} = \frac{(F_{2y} - y_{22})^2}{B_2 + (F_{2x} - x_{22})}. \qquad (13)$$

Solving system of equations (11) and (13), we arrive at

$$\begin{aligned} F_{1y} &= \frac{Y_{I2}C_u + F_{2y}Y_{I1} - y_{22}Y_{I2}}{Y_{I1} - Y_{I2} + F_{2y} - y_{22} + C_u}; \\ g_{11} &= 2\arctan\left(\frac{Y_{I2} - F_{1y}}{(Y_{I1} - F_{1y})\tan g_{12}/2}\right), \end{aligned}$$

where

$$C_u = \frac{\tan(g_{12}/2)(F_{2y} - y_{22})^2}{B_2 + (F_{2x} - x_{22})}.$$

From obvious geometric considerations,

$$\begin{aligned} F_{1x} &= X_2 + \frac{F_{1y} - y_{22}}{\tan g_{12}}; \\ y_{11} &= Y_{I1}; \\ y_{21} &= F_{2y}; \\ y_{12} &= Y_{I2}; \\ x_{11} &= F_{1x} + \frac{y_{11} - F_{1y}}{\tan g_{11}}; \\ x_{21} &= F_{1x} + \frac{y_{21} - F_{1y}}{\tan g_{11}}; \\ x_{12} &= X_1. \end{aligned}$$

The sign of $F_{1y} - Y_{I2}$ specifies the type of axicone 2:

$F_{1y} - Y_{I2} < 0 \iff$ a hyperbola;
$F_{1y} - Y_{I2} > 0 \iff$ an ellipse;
$F_{1y} - Y_{I2} = 0 \iff$ a parabola (axicone 1 being a straight line).

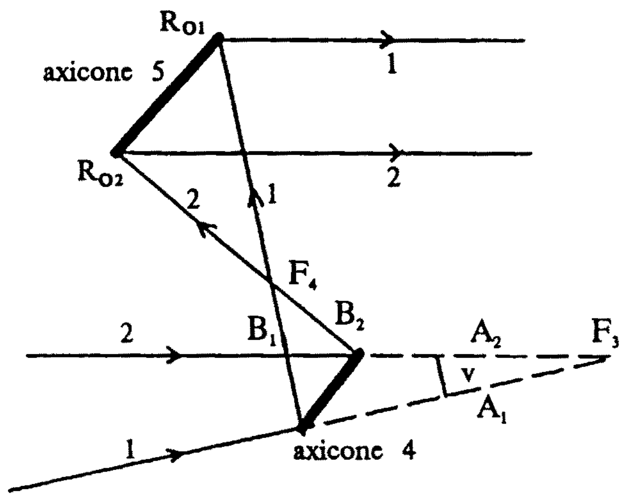

Fig. 5. Reflection of rays from axicones 4 and 5.

10. Parameters of Axicones 4 and 5

In this section, we obtain expressions for the parameters describing axicones 4 and 5 (see Fig. 5). Note that x_{41} and y_{41} were obtained previously in the calculation of axicone 3.

The location of the "personal" focus of axicone 4:

$$F_{3y} = -R_N - R_{3N};$$
$$F_{3x} = x_{41} - \frac{y_{41} - F_{3y}}{\tan v} .$$

The location of the outer edge of axicone 5:

$$y_{52} = Y_{O2};$$
$$x_{52} = x_{12} + X_{51} .$$

We introduce the notation:

A_1 and A_2 are the distances from P_{41} and P_{42} to F_3;
B_1 and B_2 are the distances from P_{41} and P_{42} to F_4.

Axicone 4 is a hyperbola, hence

$$A_2 - B_2 = A_1 - B_1.$$

Inasmuch as

$$A_1 = \sqrt{(x_{41} - F_{3x})^2 + (y_{41} - F_{3y})^2} ;$$
$$A_2 = (F_{3x} - x_{41}) - \frac{F_{4y} - y_{41}}{\tan g_{41}} + \frac{F_{4y} - F_{3y}}{\tan g_{42}} ;$$

$$B_1 = \frac{F_{4y} - y_{41}}{\sin g_{41}} ;$$
$$B_2 = \frac{F_{4y} - y_{42}}{\sin g_{42}} = \frac{F_{4y} - F_{3y}}{\sin g_{42}} ,$$

then

$$(F_{4y} - y_{41}) \left(\frac{1}{\sin g_{41}} - \frac{1}{\tan g_{41}} \right) - (F_{4y} - F_{3y}) \left(\frac{1}{\sin g_{42}} - \frac{1}{\tan g_{42}} \right) = A_1 - (F_{3x} - x_{41}).$$

In view of the identity

$$\frac{1}{\sin x} - \frac{1}{\tan x} = \frac{1 - \cos x}{\sin x} = \tan \frac{x}{2} ,$$

we obtain:

$$(F_{4y} - y_{41}) \tan \frac{g_{41}}{2} - (F_{4y} - F_{3y}) \tan \frac{g_{42}}{2} = A, \tag{14}$$

where

$$A = A_1 - (F_{3x} - x_{41}) = \frac{(F_{3y} - y_{41})^2}{A_1 + (F_{3x} - x_{41})}.$$

Using Eq. (3) we obtain for axicone 5:

$$(F_{4y} - Y_{O2}) \tan \frac{g_{42}}{2} = (F_{4y} - Y_{O1}) \tan \frac{g_{41}}{2} . \tag{15}$$

The focus F_4 is located at the intersection of rays 1 and 2. Consequently,

$$x_{41} - x_{52} = \frac{F_{4y} - Y_{O2}}{\tan g_{42}} - \frac{F_{4y} - y_{41}}{\tan g_{41}} . \tag{16}$$

Equations (14) and (15) are readily brought to the form:

$$\tan \frac{g_{41}}{2} = \frac{F_{4y} - Y_{O2}}{B} ;$$
$$\tan \frac{g_{42}}{2} = \frac{F_{4y} - Y_{O1}}{B} ,$$

where

$$B = \frac{(F_{4y} - y_{41})(F_{4y} - Y_{O2}) - (F_{4y} - F_{3y})(F_{4y} - Y_{O1})}{A} = \frac{F_{4y}(Y_{O1} - Y_{O2} + F_{3y} - y_{41}) - F_{3y}Y_{O1} + y_{41}Y_{O2}}{A} .$$

In view of these equations and the identity

$$\frac{2}{\tan x} = \frac{1}{\tan x/2} - \tan x/2,$$

relationship (16) reduces to the cubic equation

$$\Phi(F_{4y}) = C_1 (F_{4y} - y_0)^2 + 2 C_2 (F_{4y} - y_0) + C_3 = 0, \tag{17}$$

where

$$\begin{aligned}
C_1 &= C_1(F_{4y}) = F_{4y}(2Y_{O2} - Y_{O1} - y_{41}) + Y_{O1}\,y_{41} - (Y_{O2})^2;\\
C_2 &= C_2(F_{4y}) = C\,(x_{41} - x_{52})(F_{4y} - Y_{O1})(F_{4y} - Y_{O2});\\
C_3 &= C_3(F_{4y}) = C^2(y_{41} - Y_{O1})(F_{41} - Y_{O1})(F_{4y} - Y_{O2})^2;\\
C &= \frac{A}{Y_{O1} - Y_{O2} + F_{3y} - y_{41}};\\
y_0 &= \frac{F_{3y}Y_{O1} - y_{41}Y_{O2}}{Y_{O1} - Y_{O2} + F_{3y} - y_{41}}.
\end{aligned}$$

From obvious considerations, $F_{3y} < F_{4y} < Y_{O2}$. Note that C_2 does not change sign, while $C_1 < 0$ and $C_3 < 0$ in this interval.

By analyzing the change of sign of the polynomial in (17), it can be shown that cubic equation (17) has three roots: the first one is on the segment (F_{3y}, y_0); the second, on the segment (y_0, Y_{O2}); the third, outside of the segment (F_{3y}, Y_{O2}).

From obvious geometric considerations,

$$\tan\frac{g_{42}}{2} = \frac{F_{4y} - Y_{O2}}{B} = C\,\frac{F_{4y} - Y_{O2}}{F_{4y} - y_0} > 0.$$

Consequently, $F_{4y} < y_0$.

On this basis, F_{4y} is to be found on the segment (F_{3y}, y_0). The solution may be sought analytically by solving the cubic equation (see [4]) or via iterations. In our work, we used an iteration scheme similar to the method of parabolas.

As an initial approximaton, y_0 can be taken. For $C = 0$ (which corresponds to the case of $v \to 0$), the last two terms in (17) become zero and the polynomial has two roots equal to y_0. For small C, these terms are nonzero but still small when compared with the first term far from y_0. As a result, the equation has two roots close to y_0 (on the left and on the right).

Further we put

$$\begin{aligned}
C_1 &= C_1(y_0);\\
C_2 &= C_2(y_0);\\
C_3 &= C_3(y_0),
\end{aligned}$$

i.e., we approximate the cubic polynomial with a parabola. As a new approximation, we take the lesser root of the quadratic equation obtained. We repeat the iterations until the required accuracy is achieved. In the vicinity of y_0, the magnitudes of C_1, C_2, and C_3 vary ever so slowly, which promises fast convergence of the iterations.

After deriving F_{4y}, the value of x_{52} should be corrected by setting

$$x^*_{52} = x_{41} + \frac{C_1(F_{4y})(F_{4y} - y_0)^2 + C_3(F_{4y})}{2\,C_2(F_{4y})(F_{4y} - y_0)(x_{41} - x_{52})}.$$

In fact, this implies a small change in X_{51}.

11. Example of Calculation

The algorithm stated above was tested with the following initial data (the dimensions are given in millimeters):

$$R_N = 150; \quad R_L = 50;$$

TABLE 1. The Curve Parameters Describing the Surfaces of HEX-DARR Resonator

Axicone 1					
p	=	496.785 468 789 796 300	e	=	1.000 000 000 000 000
x_0	=	264.465 690 379 485 200	φ_0	=	0.000 000 000 000 000
y_0	=	712.070 453 638 987 100	φ_1	=	4.360 223 974 078 329
			φ_2	=	4.402 989 418 760 000
Axicone 2					
p	=	594.641 980 466 858 700	e	=	0.767 132 507 404 5093
x_0	=	264.465 690 379 485 200	φ_0	=	2.908 520 220 714 430
y_0	=	712.070 453 638 987 100	φ_1	=	4.360 223 974 078 329
			φ_2	=	4.402 989 418 760 000
Axicone 3					
p	=	4847.326 842 933 073 000	e	=	1.000 000 000 000 000
x_0	=	2421.581 968 800 840 000	φ_0	=	1.565 817 404 909 536
y_0	=	200.000 000 000 000 000	φ_1	=	3.140 592 653 589 793
			φ_2	=	3.152 550 497 360 514
Axicone 4					
p	=	35.219 718 309 796 850	e	=	1.015 080 232 260 482
x_0	=	117.704 695 820 373 700	φ_0	=	0.007 184 485 207 313 319
y_0	=	134.095 287 470 663 200	φ_1	=	0.901 243 483 055 800 3
			φ_2	=	1.690 558 522 186 128
Axicone 5					
p	=	116.826 373 506 591 900	e	=	1.000 000 000 000 000
x_0	=	117.704 695 820 373 700	φ_0	=	3.141 592 653 589 793
y_0	=	134.095 287 470 663 200	φ_1	=	4.042 836 136 645 593
			φ_2	=	4.832 151 175 775 922

$$Y_{I1} = 1; \quad Y_{I2} = 31;$$
$$Y_{O1} = -2.5; \quad Y_{O2} = -75.5;$$
$$X_1 = 46; \quad X_2 = 93; \quad X_3 = -2,450;$$
$$R_{24} = 4; \quad R_{3N} = 1;$$
$$X_{51} = 27; \quad X_{42} = 20.$$

Listed in Tables 1 and 2 are the parameters of the curves describing the axicones of such a resonator and

TABLE 2. The Ray Traces (the Coordinates and the Guide Vectors of Rays) in HEX-DARR Resonator

X	Y	X_n	Y_n
Entrance plane $X = -100$			
-100.000 000 00	1.000 000 00	1.000 000 00	0.000 000 00
-100.000 000 00	16.000 000 00	1.000 000 00	0.000 000 00
-100.000 000 00	31.000 000 00	1.000 000 00	0.000 000 00
Reflection from axicone 1			
3.965 530 55	1.000 000 00	0.343 991 95	0.938 972 60
25.209 221 18	16.000 000 00	0.325 058 20	0.945 694 01
46.000 000 00	31.000 000 00	0.305 439 13	0.952 211 60
Reflection from axicone 2			
76.869 040 38	200.000 000 00	-1.000 000 00	0.000 000 00
84.667 939 10	188.983 647 61	-0.999 988 89	-0.004 714 01
93.000 000 00	177.523 288 24	-0.999 953 42	-0.009 652 08
Reflection from axicone 3			
-2450.000 000 00	200.000 000 00	-0.004 978 90	-0.999 987 61
-2473.134 498 56	176.926 014 05	-0.004 978 90	-0.999 987 61
-2497.488 179 10	152.518 518 42	-0.004 978 90	-0.999 987 61
Reflection from axicone 3			
-2451.981 765 09	-198.027 678 38	0.999 954 37	0.009 553 00
-2474.887 586 92	-175.173 077 73	0.999 988 06	0.004 887 50
-2498.999 386 58	-151.000 000 00	1.000 000 00	0.000 000 00
Reflection from axicone 4			
113.000 000 00	-173.523 288 24	0.118 483 21	0.992 956 06
123.637 290 99	-162.472 646 78	-0.204 637 42	0.978 837 85
131.057 751 62	-151.000 000 00	-0.619 851 02	0.784 719 51
Reflection from axicone 5			
133.407 135 38	-2.500 000 00	1.000 000 00	0.000 000 00
97.858 834 09	-39.167 096 52	1.000 000 00	0.000 000 21
73.000 000 01	-77.499 999 99	1.000 000 00	0.000 000 00
Outlet plane $X = 100$			
100.000 000 00	-2.500 000 00	1.000 000 00	0.000 000 00
100.000 000 00	-39.167 096 06	1.000 000 00	0.000 000 21
100.000 000 00	-77.499 999 99	1.000 000 00	0.000 000 00

the ray paths going up in it. (X, Y) define the ray coordinates, and (X_d, Y_d), the direction cosines of the rays.

It is easily seen that all initial conditions are fulfilled virtually exactly. The emergent beam is parallel to the axis (its deviation does not exceed 0.05″). The fast convergence of the iterations in finding q and F_{4y} is noteworthy. It took eight iterations to calculate q with computer accuracy and seven iterations for F_{4y}. The foregoing analytical formulas for initial approximation of q proved to be highly accurate. For instance, for $q = q_0$, the discrepancy $|x_{22} - X_2| \approx 3$, while for $q = q_1$, it decreases to 0.3, which is quite small in comparison with the base resonator dimension, which is equal to 2450.

12. Summary

We underline the most important points set forth in this work.

1. We considered a class of mirrors (with surfaces formed by rotating second-order curves) which extends the range of possible beam conversions in optical systems. The formulas used in the calculations are quite simple.

2. On the basis of this approach, a complete analytical algorithm for calculating the mirror surface parameters in a HEX-DARR resonator was worked out and presented.

3. To verify the algorithm, a numerical calculation of an optical system was carried out for a specific initial data set. The results obtained confirm the accuracy of the equations derived and the efficiency of the algorithm.

References

1. Yu. A. Anan'ev, *Optical Resonators and Laser Beams*, [in Russsian], Nauka, Moscow (1990).
2. J. Liller, "High Power Hydrogen Fluoride Chemical Lasers: Power Scaling and Beam Quality," Report at the International Conference "LASERS–87" (Lake Tahoe, Nevada, USA, 7-11 December 1986).
3. G. M. Popov, *Modern Astronomical Optics* [in Russsian], Nauka, Moscow (1988).
4. G. A. Korn and T. M. Korn, *Mathematical Handbook for Scientists and Engineers*, 2nd ed., McGraw-Hill, New York (1968).